

The forkhead transcription factor *Foxo1* links insulin signaling to *Pdx1* regulation of pancreatic β cell growth

Rapid Publication

Tadahiro Kitamura,¹ Jun Nakae,¹ Yukari Kitamura,¹ Yoshiaki Kido,¹ William H. Biggs III,² Christopher V.E. Wright,³ Morris F. White,⁴ Karen C. Arden,² and Domenico Accili¹

¹Naomi Berrie Diabetes Center, Department of Medicine, College of Physicians & Surgeons of Columbia University, New York, New York, USA

²Ludwig Institute for Cancer Research, University of California San Diego, San Diego, California, USA

³Vanderbilt University Medical Center, Nashville, Tennessee, USA

⁴Joslin Diabetes Center and Howard Hughes Medical Institute, Harvard University, Boston, Massachusetts, USA

Diabetes is caused by an absolute (type 1) or relative (type 2) deficiency of insulin-producing β cells. The mechanisms governing replication of terminally differentiated β cells and neogenesis from progenitor cells are unclear. Mice lacking insulin receptor substrate-2 (*Irs2*) develop β cell failure, suggesting that insulin signaling is required to maintain an adequate β cell mass. We report that haploinsufficiency for the forkhead transcription factor *Foxo1* reverses β cell failure in *Irs2*^{-/-} mice through partial restoration of β cell proliferation and increased expression of the pancreatic transcription factor pancreas/duodenum homeobox gene-1 (*Pdx1*). *Foxo1* and *Pdx1* exhibit mutually exclusive patterns of nuclear localization in β cells, and constitutive nuclear expression of a mutant *Foxo1* is associated with lack of *Pdx1* expression. We show that *Foxo1* acts as a repressor of *Foxa2*-dependent (*Hnf-3 β* -dependent) expression from the *Pdx1* promoter. We propose that insulin/IGFs regulate β cell proliferation by relieving *Foxo1* inhibition of *Pdx1* expression in a subset of cells embedded within pancreatic ducts.

J. Clin. Invest. **110**:1839–1847 (2002). doi:10.1172/JCI200216857.

Introduction

Type 2 diabetes results from combined defects of insulin action and pancreatic β cell function (1, 2). Classically, the two abnormalities have been considered as separate entities. However, the recent demonstration that insulin/IGF signaling plays a

role in insulin secretion and β cell proliferation has led to a critical reassessment of this view (3). For example, inactivation of insulin receptor (*Insr*) (4) or IGF-1 receptor (*Igf1r*) (5, 6) leads to impaired insulin secretion, while inactivation of insulin receptor substrate-2 (*Irs2*) impairs β cell proliferation (7, 8). These observations indicate that peripheral insulin resistance and β cell failure may share a common pathogenesis. However, the mechanism by which insulin signaling regulates β cell function remains unclear. Forkhead transcription factors of the *Foxo* subfamily, previously known as *Fkhr* (9), can promote (10) or repress (11) gene expression. Insulin inhibits *Foxo* through Akt-mediated phosphorylation and nuclear exclusion, and *Foxo1* mutations affect insulin sensitivity in mice (12). Here we report the identifica-

tion of *Foxo1* as an effector of insulin action in pancreatic β cells, and propose a model in which *Foxo1* links insulin signaling to regulation of β cell mass.

Methods

Reagents. We maintained and transfected kidney epithelial cells and β cells according to standard protocols (13). We purchased anti-insulin antibody from Linco Research Inc. (St. Charles, Missouri, USA), anti-Hemagglutinin (12CA5), and anti-5-bromo-2-deoxyuridine (anti-BrdU) antibodies from Sigma-Aldrich (St. Louis, Missouri, USA); anti-c-Myc antibody (9E10) from Roche Molecular Biosystems (Indianapolis, Indiana, USA); anti-*Foxo1* and anti-phospho-*Foxo1*^{S253} from Cell Signaling Technology Inc. (Beverly, Massachusetts, USA); and anti-*Foxa2* monoclonal antibody from the Developmental Studies Hybridoma Bank at the University of Iowa (Iowa City, Iowa, USA). We described previously the anti-*Foxo1* antiserum used for gel shift assays (13) and the antibody against pancreas/duodenum homeobox gene-1 (*Pdx1*) (12). Expression vectors and *Foxo1* adenoviruses have been described previously (13). All primer sequences are available upon request.

Animal production and phenotypic analysis. We have described *Insr*, *Irs2*, and *Foxo1* mutant mice (12). We measured glucose and insulin as indicated in previous publications (12).

Real-time RT-PCR and Northern analysis of gene expression. We isolated mRNA using the Micro-Fast Track 2.0 kit (Invitrogen Corp., San Diego,

Received for publication September 9, 2002, and accepted in revised form October 22, 2002.

Address correspondence to: Domenico Accili, Berrie Research Pavilion, 1150 St. Nicholas Avenue, Room 238A, New York, New York 10032, USA.
Phone: (212) 851-5332; Fax: (212) 851-5331; E-mail: da230@columbia.edu.

Conflict of interest: The authors have declared that no conflict of interest exists.

Nonstandard abbreviations used: insulin receptor (*Insr*); IGF-1 receptor (*Igf1r*); insulin receptor substrate-2 (*Irs2*); 5-bromo-2-deoxyuridine (BrdU); pancreas/duodenum homeobox gene-1 (*Pdx1*); glucokinase (*Gck*); Fas ligand (*FasL*); Bcl-2 interacting mediator (*BimL*); secreted alkaline phosphatase (*SEAP*); β -galactosidase (β -gal).

California, USA). We carried out Northern blots according to standard methods and semiquantitative RT-PCR using the GeneAmp RNA PCR kit (Applied Biosystems, Foster City, California, USA) with amplification primers corresponding to *Foxo1*, *Foxo3*, *Foxo4*, *Pdx1*, *Irs2*, *insulin*, *glucagon*, *pancreatic polypeptide*, and *β -actin* sequences. We performed real-time PCR using primers encoding *insulin 2*, *Pdx1*, *Slc2a2*, *glucokinase (Gck)*, *Foxa2*, *Bad*, *Bcl-2 interacting mediator (BimL)*, *Fas ligand (FasL)*, and *p27^{kip}*. For these experiments, we isolated mRNA from handpicked islets of similar sizes derived from three 4-week-old animals for each genotype and amplified it using a LightCycler PCR instrument and LightCycler RT-PCR kit (Roche Molecular Biosystems). We carried out each reaction in triplicate using a standard curve with the relevant cDNA for each primer set.

Immunohistochemical and morphometric analysis of pancreatic islets. We isolated and fixed pancreata from 8-week-old wild-type, *Irs2*^{-/-}, *Irs2*^{-/-}*Insr*^{+/-}, and *Irs2*^{-/-}*Foxo1*^{+/-} mice overnight in 2% paraformaldehyde solution, embedded them in paraffin, and immunostained consecutive 5- μ m sections for β and α cells using anti-insulin and anti-glucagon antibodies, respectively. We performed morphometry using NIH Image 1.60 software (NIH, Bethesda, Maryland, USA) as described (14). We expressed results as percentage of total surveyed pancreatic area occupied by β and α cells.

Immunofluorescence. We incubated frozen islet sections with anti-insulin, anti-Pdx1, and anti-Foxo1 antibodies at dilutions of 1:1,000, 1:5,000 and 1:30, respectively. We visualized immune complexes using a CY3-conjugated anti-guinea pig IgG for anti-insulin antiserum, and FITC-conjugated secondary anti-rabbit IgG for anti-Pdx1 and anti-Foxo1 antisera. For colocalization of Foxo1 and Pdx1, we costained two adjacent sections with insulin and Pdx1, or insulin and Foxo1 antibodies, respectively. Thereafter, we acquired images using a SPOT-RT digital camera (Morrill Instruments, Melville, New York, USA) and identified matching

islets in the two sections by overlaying the insulin immunostaining. We rendered Pdx1 immunoreactivity as mauve pseudocolor and scored cells in which we could unambiguously identify the nucleus on both sections for either Pdx1 or Foxo1 immunoreactivity. We analyzed a total of ten sections and 50 islets from three mice for each genotype. We fixed transfected β TC-3 cells in 2% paraformaldehyde and permeabilized them in 0.2% Triton X-100 for immunofluorescence as described previously (13). We visualized endogenous Pdx1 with anti-Pdx1 polyclonal antibody and FITC-conjugated anti-rabbit IgG. We detected transiently expressed c-Myc-Foxo1 in the same sections with a monoclonal anti-c-Myc antibody followed by CY3-conjugated anti-mouse IgG.

Detection and quantitation of β cell replication. We injected BrdU intraperitoneally (0.1 g/kg) into 2-week-old wild-type, *Irs2*^{-/-}, and *Irs2*^{-/-}*Foxo1*^{+/-} mice. After 4 hours, we removed and fixed pancreata in PBS (pH 7.4) containing 2% paraformaldehyde and embedded them in paraffin. We immunostained the sections with mouse anti-BrdU antibody (1:1,000). We incubated the sections sequentially with biotinylated anti-mouse IgG reagent (Vector Laboratories Inc., Burlingame, California, USA), VECTASTAIN Elite ABC reagent and DAB (Vector Laboratories Inc.) for visualization. For double staining with anti-BrdU and anti-insulin antibodies, we used a guinea pig anti-insulin antibody. We performed quantitation of β cell and acinar cell replication by counting cells in more than 50 islets stained with anti-insulin antibody for each genotype (for BrdU-labeled β cells) and more than 50 different exocrine fields for each genotype (for BrdU-labeled exocrine cells). We expressed the results as a "labeling index," i.e., percentage of total cells in surveyed islets and exocrine fields that were BrdU-positive.

Luciferase and secreted alkaline phosphatase assays. The sequence used for these experiments spanned nucleotides -2,233 to -2,097 of the *Pdx1* promoter and includes a single consensus

forkhead binding site (15). We carried out cotransfections in β TC-3 cells at 70–80% confluence with *Pdx1*/luciferase reporter gene (pGL3-PDX1-PH2) and control pCMV5 vector or pCMV5-*Foxa2*, pCMV5-ADA-*Foxo1*, and pCMV5-wild-type *Foxo1*. We used secreted alkaline phosphatase (SEAP) (20 ng) as a control for transfection efficiency. We measured luciferase and SEAP activity according to the manufacturer's specifications (Great EscAPE SEAP kit; Clontech Laboratories Inc., Palo Alto, California, USA). In cotransfection experiments, we added recombinant adenovirus encoding ADA-*Foxo1* to cells at different moi's 12 hours after transfection with *Foxa2*. Forty-eight hours later, we determined luciferase activity in triplicate samples and normalized it by SEAP activity.

Gel shift assays. We isolated nuclei of LLC or β TC-3 cells by sequential extraction in NaCl (16). In some experiments, we transduced cells with Foxo1 adenovirus 48 hours prior to nuclei isolation. We incubated double-stranded ³²P-labeled oligonucleotide probes (20,000 cpm; 5 fmol) corresponding to the consensus forkhead binding region in the *Pdx1* PH2 domain (5'-AGTGCTAAGCAAACATCCTG-3') with nuclear extracts for 20 minutes at room temperature in the presence of 10 mM Tris-HCl (pH 7.5), 50 mM NaCl, 1 mM MgCl₂, 0.5 mM EDTA, 4% glycerol, 0.5 mM DTT, and 100 ng of poly(dI-dC) \times poly(dI-dC). For competition experiments, we used either the wild-type oligonucleotide indicated above, or a mutant oligonucleotide: 5'-AGTGCTAcGCcggtgTCCCTG-3' (mutant nucleotides are in lower case). The concentrations of cold competitor used were 0, 100-, 300- and 900-fold excess for both wild-type and mutant probes. We resolved the DNA/protein complexes on 6% non-denaturing polyacrylamide gel and visualized them by autoradiography. For supershift experiments, we incubated anti-Foxa2, anti-Foxo1, or non-immune sera with nuclear extracts for 10 minutes at room temperature. We incubated competitor wild-type and mutant probes in the reaction mixture for 10 minutes prior to the addition of the radiolabeled probe.

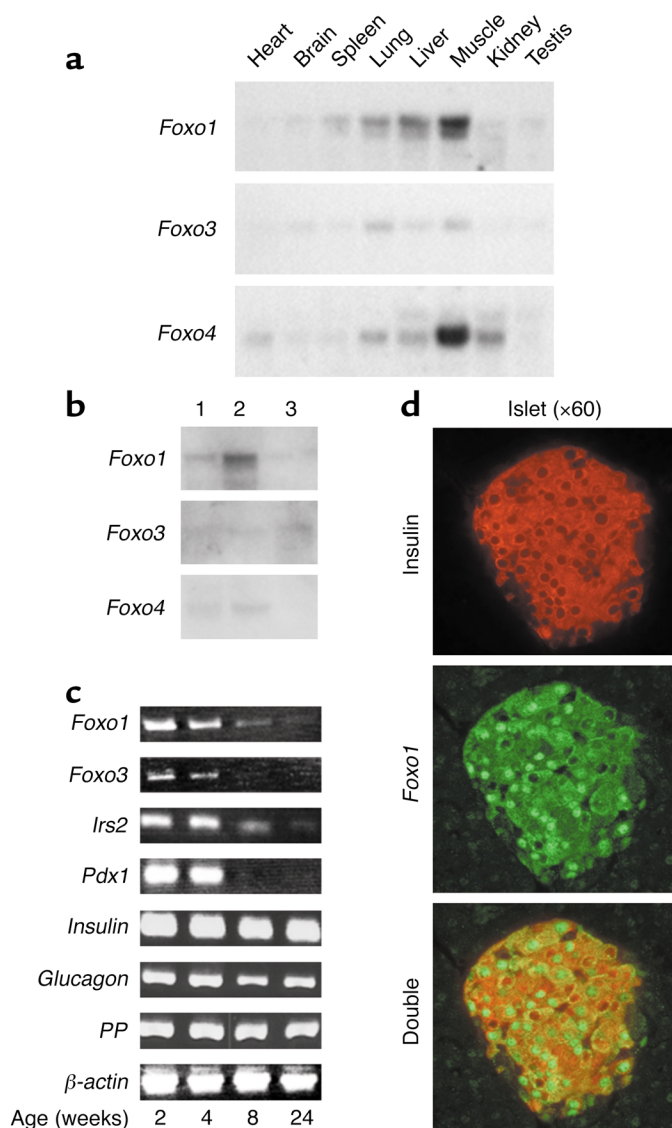


Figure 1

(a) Tissue survey of *Foxo* isoform expression in mice. We hybridized multiple tissue Northern blots (filter membranes; Clontech Laboratories Inc.) with probes encoding the three *Foxo* isoforms, labeled with ^{32}P at similar specific activities to obtain readily comparable hybridization signals. (b) *Foxo1* expression in cultured β cells. We isolated mRNA from SV40-transformed mouse hepatocytes (lane 1), $\beta\text{TC-3}$ (lane 2), and HEK293 cells (lane 3), and performed Northern blot analysis using specific probes for *Foxo1*, *Foxo3*, and *Foxo4*. (c) Time course analysis of *Foxo1* expression in islets. We isolated mRNA from islets of wild-type mice at 2, 4, 8, and 24 weeks of age. We performed RT-PCR using primers for *Foxo1*, *Foxo3*, *Foxo4* (not shown, because no amplification could be seen), *Irs2*, *Pdx1*, *insulin*, *glucagon*, *pancreatic polypeptide*, and β -actin as indicated in Methods. (d) Islet immunohistochemistry. We performed double immunohistochemistry with anti-*Foxo1* and anti-insulin antisera on the same section to localize *Foxo1* expression. We visualized the anti-insulin antibody with CY3-conjugated anti-guinea pig IgG, and the anti-*Foxo1* with FITC-conjugated anti-rabbit IgG.

Results

RNA expression studies indicate that the three *Foxo* isoforms differ with respect to tissue localization, with *Foxo1* representing the predominant mRNA isoform in liver (17), lung, and spleen, and *Foxo4* in heart, skeletal muscle, and kidney (13). *Foxo3* mRNA distribution mirrored that of *Foxo1*, albeit at lower levels (Figure 1a). *Foxo1* is also the main member of the *Foxo* subfamily in cultured β cells ($\beta\text{TC-3}$ line) (Figure 1b, lane 2) and murine islets. Its levels decline over the first 6 months of life, as do *Irs2* and *Pdx1* levels. *Foxo3* is expressed at lower levels and *Foxo4* is undetectable in islets (not shown). Although a decrease in *Pdx1* expression with age has been reported in rat islets (18), the present

observation suggests that the downregulation of *Pdx1* mRNA occurs earlier than previously thought. It remains to be seen, however, whether this is a specific difference between rats and mice or a reflection of inter-strain variability in mice. Immunohistochemistry of pancreatic islets with anti-*Foxo1* and anti-insulin antisera demonstrates colocalization of *Foxo1* and insulin to β cells. The subcellular localization of *Foxo1* in β cells is heterogeneous, with some cells showing exclusive cytoplasmic or nuclear immunoreactivity, and some cells showing diffuse immunoreactivity (Figure 1d).

To address whether *Foxo1* participates in β cell function, we tested the ability of a loss-of-function *Foxo1*

mutation to rescue β cell failure in *Irs2*^{-/-} mice by crossing *Irs2*^{-/-} and *Foxo1*^{+/-} mice (12). In *Irs2*^{-/-} mice, insulin-immunoreactive β cell area was about 70% smaller than in the wild-type at 8 weeks of age (Figure 2, a and b), with only a slight decrease in glucagon-immunoreactive α cell area (Figure 2b). No changes were observed in *Foxo1*^{+/-} mice (12). In contrast, in *Irs2*^{-/-}*Foxo1*^{+/-} mice, β cell area was restored to about 80% of wild-type values. *Irs2*^{-/-}*Foxo1*^{+/-} mice have a normal life span and do not develop diabetes (Table 1).

Akt-dependent phosphorylation inhibits *Foxo1* activity. When *Foxo1* was expressed in islets from *Irs2*^{-/-} mice by adenoviral transduction, phosphorylation of the “gatekeeper”

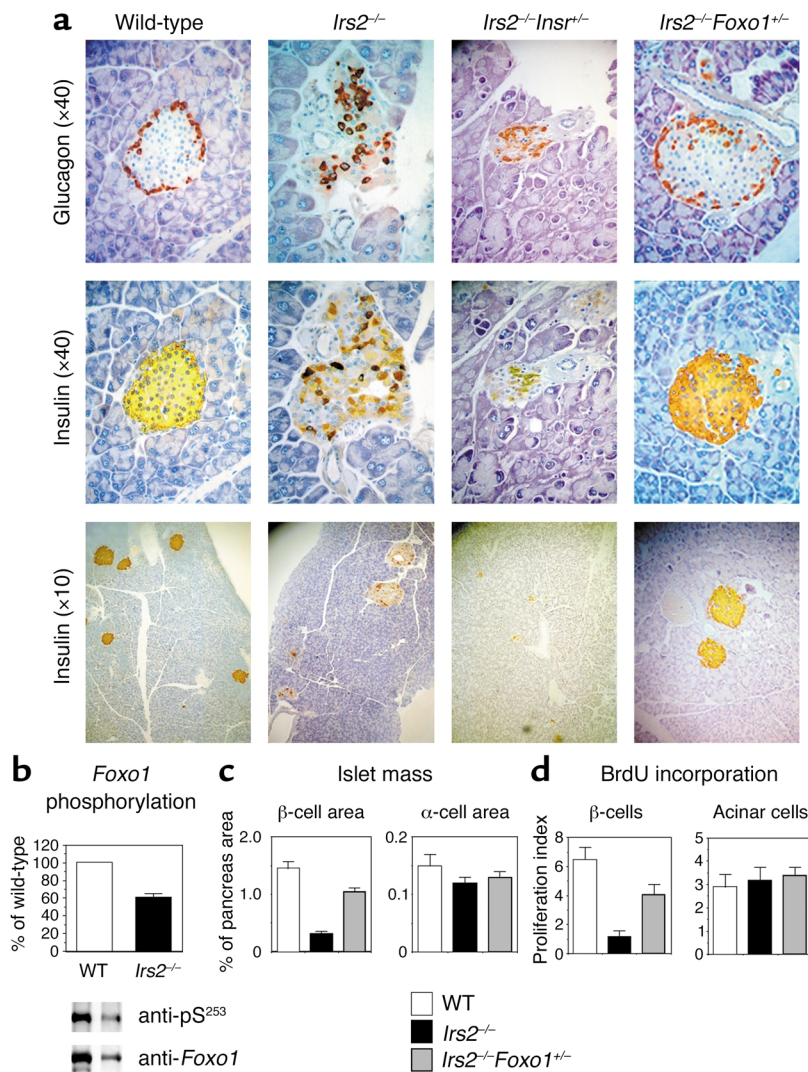


Figure 2

(a) Pancreatic histology in mice with targeted null alleles of *Irs2* and *Foxo1*. We stained pancreatic sections from 8-week-old mice of the indicated genotypes with anti-insulin and anti-glucagon antibodies. (b) *Foxo1* phosphorylation in *Irs2*^{-/-} islets. We transduced islets from wild-type and *Irs2*^{-/-} mice with adenovirus encoding hemagglutinin-tagged wild-type *Foxo1*. Following immunoprecipitation with anti-hemagglutinin antibody, we carried out immunoblotting with anti-phospho-*Foxo1*^{S253}. We then stripped and reprobed the blots with anti-*Foxo1* antibody. One of three experiments is shown, and mean phosphorylation ± SEM is summarized in the graph above (WT, white bar; *Irs2*^{-/-}, black bar), following scanning densitometry and normalization for total *Foxo1* protein levels. (c) Islet morphometry. We quantitated β and α cell area in mice of the indicated genotypes using NIH Image 1.60 analysis software. Results are expressed as the percentage of total surveyed area containing insulin- or glucagon-immunoreactive cells. (d) Measurements of mitotic indices in pancreatic cells. We labeled cells traversing S phase of the replication cycle with BrdU in vivo and visualized them in pancreatic sections using double immunohistochemistry with anti-BrdU and anti-insulin antibodies. We calculated labeling indices by counting BrdU-positive cells as percentage of total number of cells within each microscopic field. We scored exocrine acinar cells based on their morphological appearance. Results represent the mean ± SEM of 12 sections from at least four mice for each genotype. For each genotype, we scored at least 50 microscopic fields.

Akt site at serine 253 was decreased by approximately 40% compared with wild-type islets (Figure 2b), suggesting that *Foxo1* is in the *Irs2* signaling pathway. Since insulin receptor signaling inhibits *Foxo1*, we tested the effect of a loss-of-function *Insr* mutation on diabetes in *Irs2*^{-/-} mice. We generated recombinant congenic mice carrying *Irs2* and *Insr* targeted null alleles on the same chromosome (the two genes are about 4 Mb apart near the centromeric end of chromosome 8; ref. 19), and intercrossed them to produce *Irs2*^{-/-}*Insr*^{+/-} mice. *Insr* haploinsufficiency increased the severity and accelerated the onset of diabetes in *Irs2*^{-/-} mice. *Irs2*^{-/-}*Insr*^{+/-} mice developed diabetes at 6–8 weeks (Table 1) and invariably died by 10 weeks of age. Pancreatic islets were virtually undetectable by 8 weeks

(Figure 2a). Withers and colleagues have reported a similar phenotype in *Irs2*^{-/-}*Igf1r*^{+/-} mice (20).

To distinguish between increased cell proliferation and decreased apoptosis as mechanisms of β cell restoration in *Irs2*^{-/-}*Foxo1*^{+/-} mice, we measured BrdU incorporation and DNA fragmentation. BrdU incorporation was reduced by about 85% in islets of 2-week-old *Irs2*^{-/-} mice and was restored to approximately 67% of wild-type in *Irs2*^{-/-}*Foxo1*^{+/-} mice ($P < 0.05$ by ANOVA). We observed no changes in exocrine acinar tissue (Figure 2c). In contrast to proliferation, we failed to detect apoptotic cells in any of the genotypes examined using TUNEL staining at ages 2, 3, and 4 weeks (data not shown). These data indicate that restoration of β cell mass in *Irs2*^{-/-}*Foxo1*^{+/-} mice is due to increased

proliferation, rather than decreased apoptosis. Nevertheless, given that apoptosis in β cells is difficult to document (21), we cannot rule out its contribution to the observed phenotype.

Unlike β cell mass, *Foxo1* haploinsufficiency did not affect glucose-stimulated insulin secretion from islets of *Irs2*^{-/-}*Foxo1*^{+/-} mice, nor did overexpression of wild-type or mutant *Foxo1* affect insulin secretion in cultured βTC-3 cells (data not shown).

To examine the mechanism by which *Foxo1* haploinsufficiency prevents diabetes in *Irs2*^{-/-} mice, we analyzed expression of *Foxo1* target genes. They include the cell cycle inhibitor *p27^{kip}* (22) and the proapoptotic genes *FasL* (23) and *BimL* (24). For these experiments we used islets of similar size derived from 4-week-old mice to exclude artifacts due to loss of β cells.

Table 1
Metabolic characteristics of 8-week-old mice

Genotype	Body weight (g)	Glucose (fasting)	Glucose (fed)	Insulin (fasting)	Insulin (fed)
Wild-type (<i>n</i> = 13)	33.1 ± 0.6	96 ± 3	123 ± 5	0.9 ± 0.1	2.8 ± 0.2
<i>Irs2</i> ^{-/-} (<i>n</i> = 14)	31.2 ± 0.7	98 ± 4	191 ± 13 ^A	2.0 ± 0.3	4.5 ± 0.4
<i>Irs2</i> ^{-/-} <i>Foxo1</i> ^{+/-} (<i>n</i> = 14)	31.8 ± 0.6	98 ± 4	157 ± 9	1.3 ± 0.1	4.4 ± 0.4
<i>Irs2</i> ^{-/-} <i>Insr</i> ^{-/-} (<i>n</i> = 10)	29.4 ± 0.4	250 ± 13 ^A	440 ± 28 ^A	0.4 ± 0.1	1.1 ± 0.1

^A*P* < 0.05 by one-factor ANOVA compared with wild-type.

However, real-time RT-PCR analysis of islet RNA failed to detect differences in *Bad*, *BimL*, and *FasL*, while *p27*^{kip} was decreased by 40% in *Irs2*^{-/-} mice and by 30% in *Irs2*^{-/-}*Foxo1*^{+/-} mice (Figure 3), which is inconsistent with the possibility that *Foxo1* inhibits β cell replication by increasing *p27*^{kip}. Thus, changes in the expression of these genes do not appear to play a role in the observed phenotype. These data were confirmed by experiments in β TC-3 cells, in which a dominant-negative (δ 256) *Foxo1* adenovirus failed to inhibit *p27*^{kip}, *FasL*, and *BimL* expression (data not shown).

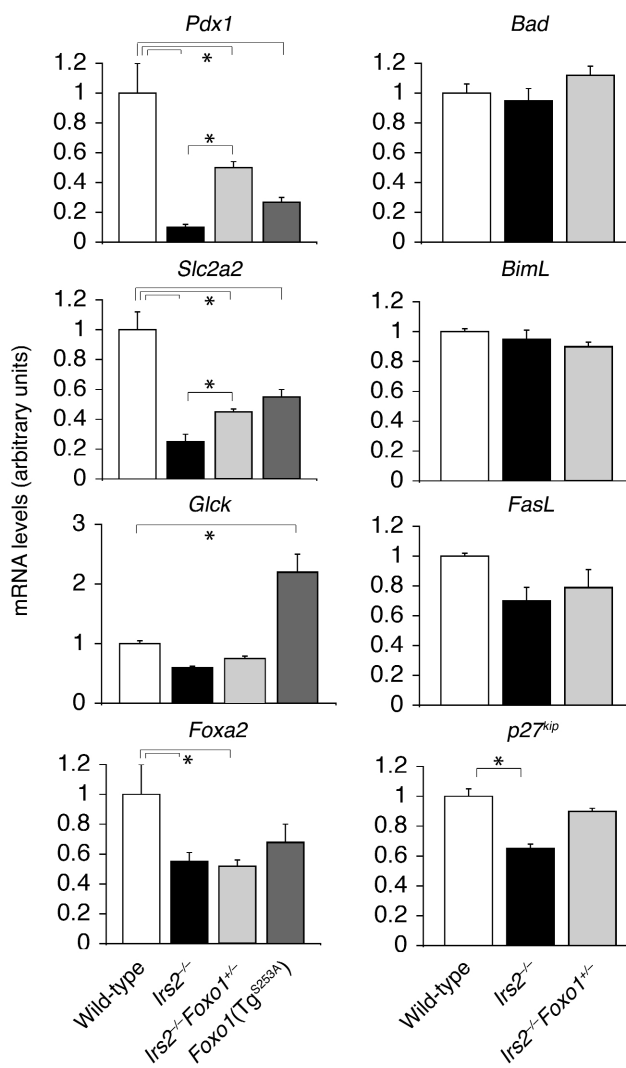
In contrast, real-time RT-PCR demonstrated a greater than 80% decrease in the expression of *Pdx1* and its target gene *Slc2a2* (glucose transporter *Glut2*) in *Irs2*^{-/-} mice. The decrease was also observed in islets of transgenic mice bearing a phosphorylation-defective *Foxo1*^{S253A} mutant in β cells (12), and was partially reversed in *Irs2*^{-/-}*Foxo1*^{+/-} mice to about 50% of wild-type. Lesser changes (~50%) were observed in *Gck* levels, consistent with two recent studies showing that *Gck* is less sensitive than *Slc2a2* to reduction of *Pdx1* expression (25, 26). In contrast, *Gck* expression was increased about twofold in *Foxo1*^{S253A} transgenics (Figure 3). The reasons for the differential regulation of *Gck* and *Slc2a2* in *Irs2*^{-/-} and *Foxo1*^{S253A} mice are unclear. *Foxa2* expression was also decreased by about 50% in *Irs2*^{-/-} and *Foxo1*^{S253A} mice, but was not restored in *Irs2*^{-/-}*Foxo1*^{+/-} islets.

Figure 3
Foxo1 haploinsufficiency restores *Pdx1* expression in β cells of *Irs2*^{-/-} mice. Real time RT-PCR analysis of gene expression. We isolated mRNA from islets and amplified it with primers encoding the genes indicated above each graph. An asterisk indicates a statistically significant difference (*P* < 0.05 by ANOVA) between genotypes.

We next compared *Pdx1* expression by immunohistochemistry. In wild-type islets, more than 95% of insulin-immunoreactive cells scored (793 of 827) were *Pdx1*-positive (Figure 4a, green). In *Irs2*^{-/-} mice, the percentage of *Pdx1*-positive cells decreased to 38.7% (245 of 632); moreover, *Pdx1* was frequently mislocalized to the cytoplasm. In *Irs2*^{-/-}*Foxo1*^{+/-} mice, the percentage of *Pdx1*-positive cells was restored to greater than 90% (678 of 730) (*P* < 0.001 by ANOVA). These data support the real-time PCR analysis

and suggest a negative correlation between *Foxo1* activity and *Pdx1* expression levels.

To investigate this relationship further, we analyzed the subcellular distribution of *Foxo1* in *Pdx1*-positive and *Pdx1*-negative β cells. Because the anti-*Foxo1* and anti-*Pdx1* antisera available for immunohistochemistry have been raised in rabbits, we could not perform double staining on the same tissue section. Therefore, we stained adjacent sections with anti-*Foxo1* and anti-insulin, or anti-*Pdx1*



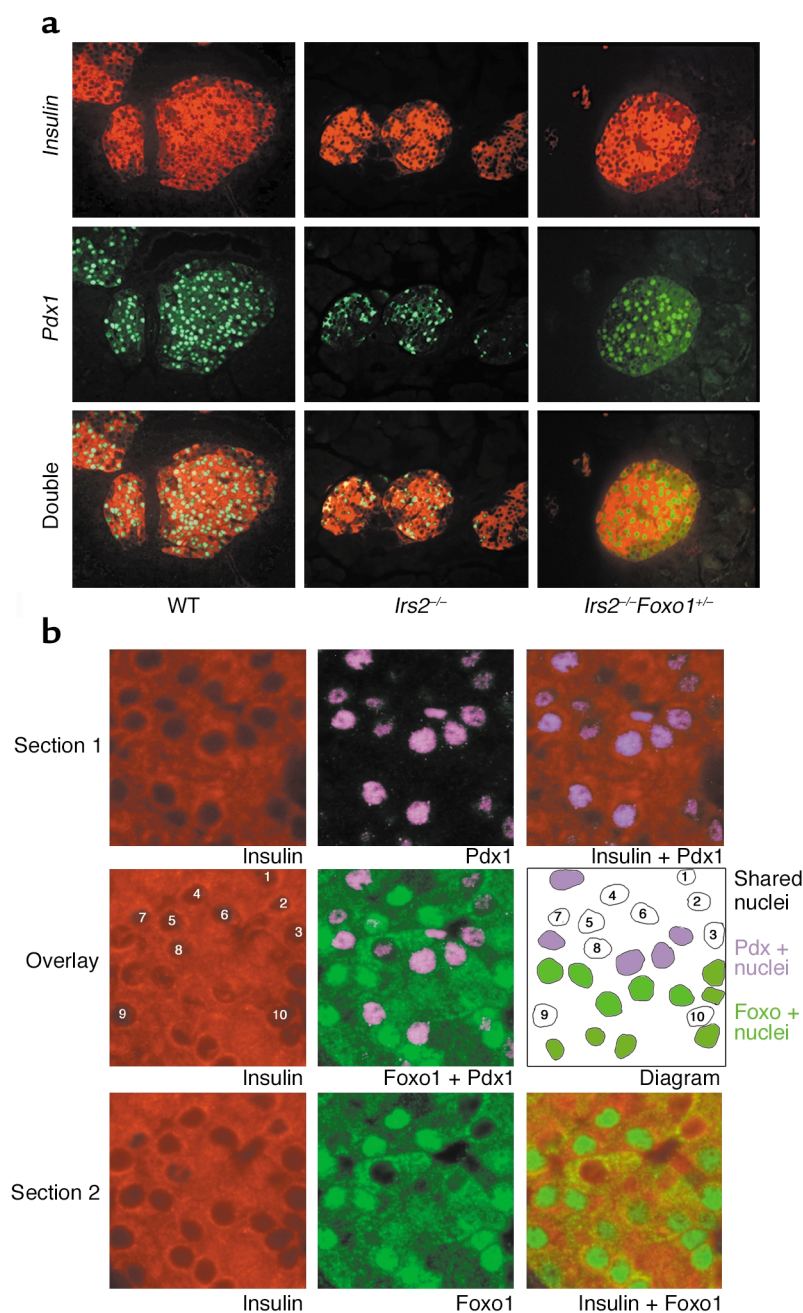


Figure 4

(a) Immunohistochemical analysis of Pdx1 expression in β cells of wild-type, *Irs2*^{-/-}, and *Irs2*^{-/-}*Foxo1*^{+/-} mice. We costained pancreatic sections with anti-Pdx1 (green) and anti-insulin antibodies (red). We show a representative section. (b) Subcellular localization of Foxo1 in Pdx1-positive and Pdx1-negative β cells from wild-type mice. We double-stained adjacent pancreatic sections from 2-week-old mice with antisera against insulin (red) and Pdx1 (mauve pseudocolor), or insulin (red) and Foxo1 (green). We acquired images using a SPOT-RT digital camera and overlaid them using the insulin-stained sections to match the position of the same nucleus in the two sections. Thereafter, we analyzed the colocalization of Pdx1 and Foxo1. We show a $\times 60$ magnification. In the schematic diagram, an empty circle indicates an overlapping nucleus in the two sections. These nuclei have been numbered to facilitate identification of matching cells in the two sections. A mauve nucleus indicates exclusive Pdx1 immunoreactivity; a green nucleus, exclusive Foxo1 immunoreactivity.

type Foxo1 was basally phosphorylated (data not shown) and was localized to the cytoplasm of Pdx1-expressing cells. In contrast, cells expressing the ADA-Foxo1 mutant in the nucleus were Pdx1-negative (Figure 5a). Moreover, we have previously shown that expression of a similar constitutively nuclear Foxo1 mutant in islets of transgenic mice results in greatly decreased Pdx1 levels (12).

In summary, *Pdx1* levels decreased in three models of increased Foxo1 activity: *Irs2*^{-/-} mice, in which Foxo1 phosphorylation is decreased (Figure 2b); transgenic mice expressing the phosphorylation-defective, constitutively nuclear Foxo1^{S253A} in β cells (12); and β TC-3 cells transduced with ADA-Foxo1 adenovirus. Conversely, *Foxo1* haploinsufficiency partially reverses the decrease in *Pdx1* levels in *Irs2*^{-/-} mice. These data support the hypothesis that Foxo1 inhibits *Pdx1* and are consistent with the observation that overexpression of Pdx1 rescues diabetes in *Irs2*^{-/-} mice (27).

To determine potential sites of interaction between Foxo1 and Pdx1, we surveyed pancreatic *Foxo1* expression. The targeting vector used to ablate *Foxo1* function contains a β -galactosidase (β -gal) cassette fused in-frame with *Foxo1* exon 1 to enable detection of

and anti-insulin antisera and carefully matched the position of β cells using insulin immunostaining to outline the nuclear margins (Figure 4b). On average, approximately 30% of cells showed matching nuclear “ghosts” in two adjacent 5- μ m sections, consistent with the fact that the average β cell diameter is 10 μ m and the nucleus occupies about 70% of the cell surface (6). In the vast majority of this subset of cells, Pdx1 and Foxo1 showed mutually exclusive nuclear localization. Thus, in approximately 80% of

Pdx1-positive cells examined, Foxo1 localized to the cytoplasm (Figure 4b, cells 1, 2, 7, and 8). By contrast, in about 80% of Pdx1-negative cells, Foxo1 localized to the nucleus (Figure 4b, cells 3, 4, 6, and 9). In addition, the occasional double-positive cells (such as cell 10 in Figure 4b) showed very weak Pdx1 immunoreactivity. These correlative findings were investigated further by expressing wild-type or a phosphorylation-defective Foxo1 mutant (ADA-Foxo1) that is constitutively nuclear (13) in β TC-3 cells. Wild-

Foxo1 expression using X-gal reactivity (12). Using this technique, we detected occasional *Foxo1*-positive cells in pancreatic ducts and exocrine acini, in addition to islets (Figure 5b, top row). In view of the potential role of duct-associated cells in β cell neogenesis, we investigated the colocalization of *Foxo1* with insulin and *Pdx1* in duct-associated cells. The majority of duct-associated *Foxo1*-positive cells did not display insulin or *Pdx1* immunoreactivity (Figure 5b, red arrows). However, all the insulin/*Pdx1*-positive duct-associated cells were *Foxo1*-positive (Figure 5b, black arrows). These data are consistent with the possibility that *Foxo1* regulates *Pdx1* expression in duct-associated cells.

Next, we used gel shift and reporter gene assays to test the hypothesis that *Foxo1* binds directly to the *Pdx1* promoter and inhibits its transcription. A 6.5-kbp *Pdx1* promoter contains elements required for β cell-specific expression, including three potential forkhead binding sites (15, 28, 29).

Among the forkhead proteins, *Foxa2* is a known activator of *Pdx1*, and *Pdx1* expression is blunted in mice lacking *Foxa2* in β cells (30). We carried out gel shift assays using nuclear extracts from LLC (Figure 6a) and β TC-3 cells (Figure 6b). When we used a probe carrying the proximal consensus forkhead binding site of the *Pdx1* promoter (PH2 domain) (15), we detected a gel retardation complex that could be competed for by excess cold probe, but not by a mutant probe (Figure 6a). In insulin-producing β TC-3 cells, we detected at least two gel retardation complexes, indicated as I and II. Addition of anti-*Foxo1* antiserum caused a supershift to yield a distinct complex III. Addition of anti-*Foxa2* monoclonal antibody caused a supershift of complex A to yield complex IV. Addition of nonimmune serum did not cause any supershift (Figure 6b).

We used cotransfection assays with a minimal *Pdx1* promoter containing the proximal *Foxa2* binding site to

study the effect of *Foxo1* in *Pdx1* transcription. Expression of *Foxa2* increased *Pdx1*/luciferase activity approximately tenfold, whereas *Foxo1* failed to do so (Figure 6c). Coexpression of constitutively active *Foxo1* inhibited *Foxa2*-dependent *Pdx1* transcription in a dose-dependent manner up to about 60%, consistent with the possibility that *Foxo1* acts as a transrepressor of *Foxa2*-dependent *Pdx1* transcription (Figure 6d). The ability of *Foxo1* to inhibit *Foxa2*-dependent *Pdx1* transcription was not due to the presence of an excess of *Foxo1* protein, since we detected the inhibitory effect when *Foxa2* levels exceeded those of *Foxo1* (Figure 6e). We obtained similar data when we used the full-length *Pdx1* promoter construct (data not shown). These data provide proof of principle that *Foxo1* can act as a repressor of *Pdx1* transcription in a transfection system. However, it is likely that the in vivo interaction between *Foxo1* and *Pdx1* is complex, and

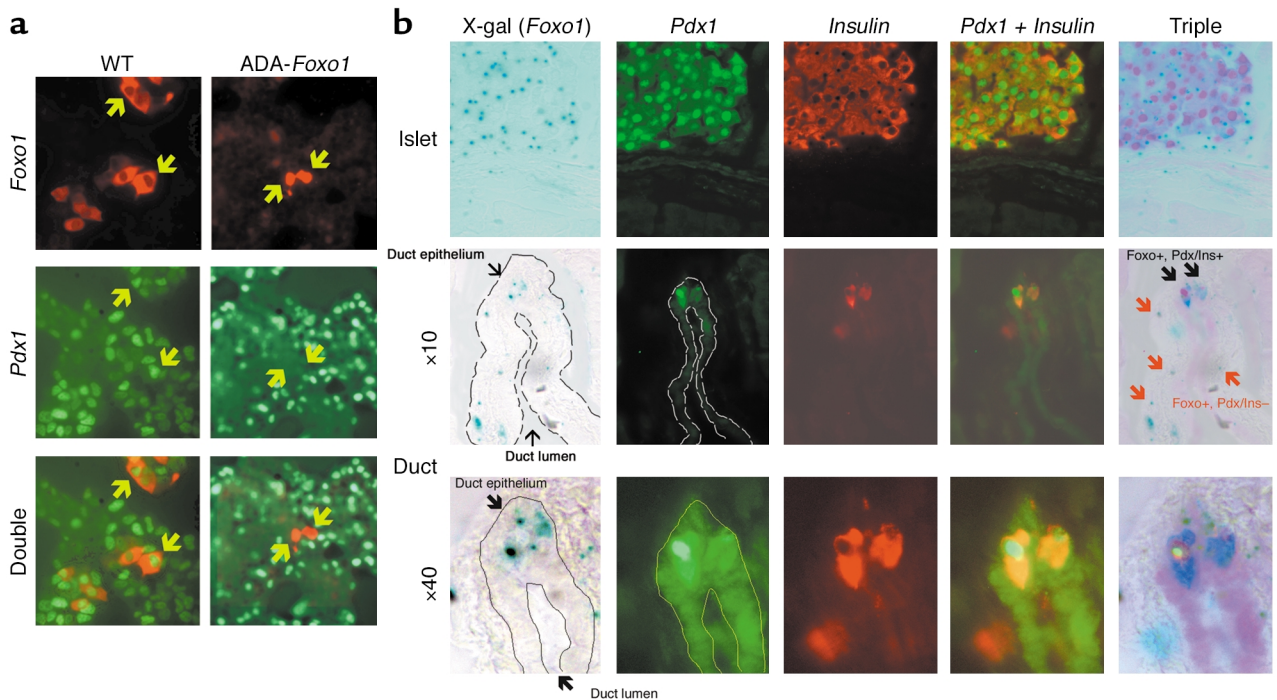


Figure 5

(a) *Pdx1* expression in β TC-3 cells transfected with c-Myc-tagged wild-type (left column) or ADA-*Foxo1* (right column). We performed immunocytochemistry with anti-c-Myc (top row) and anti-*Pdx1* (middle row). We visualized anti-c-Myc immunoreactivity with CY3-conjugated anti-mouse IgG (red) and anti-*Pdx1* immunoreactivity with FITC-conjugated anti-rabbit IgG (green). We show double staining in the bottom row. (b) *Foxo1* localization in pancreatic duct-associated cells. We treated frozen sections for immunohistochemistry with anti-insulin and anti-*Pdx1* antisera, followed by incubation in X-gal to detect β -gal expression from the *Foxo1* locus. In the top row, we show a representative endocrine islet, demonstrating that X-gal reactivity colocalizes with islets. Occasional X-gal-positive cells can also be visualized in ducts and acini. In the middle and bottom rows, we show that X-gal reactivity in ducts can be detected in cells that do not express insulin and/or *Pdx1* (red arrows), as well as cells with insulin and *Pdx1* immunoreactivity (black arrows).

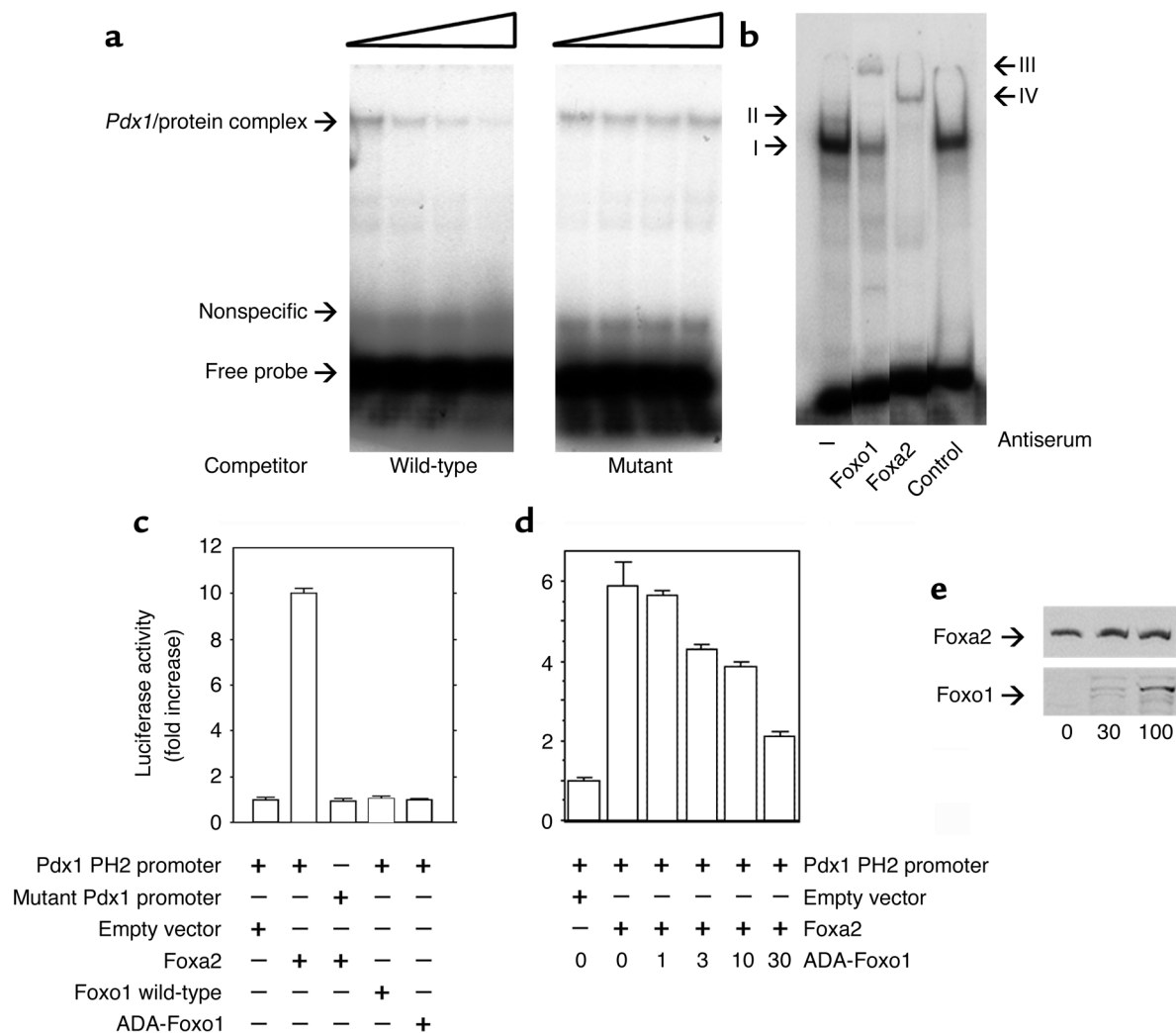


Figure 6

Foxo1 binds to the *Pdx1* promoter and inhibits Foxa2-induced *Pdx1* transcription. (a and b) Gel shift assays. (a) We used nuclear extracts from kidney epithelial LLC cells transduced with Foxo1 adenovirus to test the specificity of binding to the *Pdx1* probe. We chose this cell type because it does not express Foxa2 (13), which is abundant in β TC-3 cells. The concentrations of cold competitor used are indicated by the triangle and are 0, 100-, 300-, and 900-fold excess for both wild-type and mutant probes. (b) Antisera-induced supershift. We incubated β TC-3 nuclear extracts with antisera against Foxo1 and Foxa2 or with nonimmune serum (control). I and II correspond to the two main complexes detected in the absence of antiserum, III and IV to the supershifted complexes. (c) Foxa2, but not Foxo1, induces *Pdx1* promoter activity. We cotransfected β TC-3 cells with the plasmids indicated at the bottom of the graphs. After 48 hours, we measured luciferase activity and normalized it by SEAP activity relative to the basic pCMV5 vector. (d) Foxo1 inhibits Foxa2-dependent *Pdx1* transcription. We cotransfected β TC-3 cells with the *Pdx1*-luciferase reporter gene and pCMV5 vector or pCMV5-Foxa2. Five hours after transfection, cells were transduced with control adenovirus or with adenovirus encoding ADA-Foxo1 at the indicated moi. After 36 hours, we measured relative luciferase activity. (e) We determined immunoreactive Foxo1 and Foxa2 levels by Western blotting in cells transduced with Foxo1 at different mois. Foxo1 was not detectable by this approach in untransduced cells because of its low expression levels.

depends on the relative abundance of Foxo1, the contributions of coactivators and corepressors, and signals regulating Foxo1 localization.

Discussion

Our genetic analysis indicates that *Foxo1* is an effector of *Irs2* signaling in pancreatic β cells. *Foxo1* inactivation leads to increased *Pdx1* expression and β cell proliferation. Since *Foxo1* is expressed in a subset of cells embed-

ded within pancreatic ducts, we propose that, in quiescent duct-associated cells that are not committed to a β cell fate, *Foxo1* acts as a transcriptional brake on *Pdx1*. We propose the following mechanism of *Foxo1* regulation: small quantities of insulin are released in the pancreatic duct (31), where they activate signaling (32) in the Foxo1-positive duct cell subset, leading to Foxo1 nuclear exclusion and *Pdx1* expression. In this hypothesis, pancre-

atic islets of Langerhans are functionally associated with ducts. While controversial (33), this assumption is supported by a recent reassessment of the functional anatomy of the pancreas, showing that most islets are associated with pancreatic ducts and providing a morphological correlate for insulin release into pancreatic ducts (34). The implication of this model is that insulin is the main promoter of islet proliferation in hyperinsulinemic,

insulin-resistant patients, and that insulin resistance predisposes to β cell failure via impaired Foxo1 phosphorylation. This model provides a unifying hypothesis for the commonest abnormalities of type 2 diabetes: peripheral insulin resistance and impaired β cell compensation. Furthermore, it suggests that acute islet destruction in type 1 diabetes prevents significant islet regrowth, because there is no insulin to stimulate ductal neogenesis. This hypothesis is consistent with the observation that insulin administration following streptozotocin-induced β cell ablation is associated with robust islet regrowth (35, 36). Whether this mechanism is physiologically relevant in the context of ongoing autoimmunity is an open question. Finally, the notion that β cell neogenesis from a subset of duct-associated cells is a compensatory response to insulin resistance, rather than a physiologic event, reconciles the proposed role of ductal neogenesis (37) with the recent demonstration that duct epithelial cells do not physiologically give rise to endocrine cells (38). We propose that *Foxo1* is an important target for the development of drugs that improve β cell proliferation.

Acknowledgments

This work was supported by NIH grant DK-57539 and Juvenile Diabetes Research Foundation grant 200-893 (to D. Accili). T. Kitamura is the recipient of a Juvenile Diabetes Foundation Postdoctoral Fellowship. We thank N. Fleischer for the gift of β TC-3 cells, and Y. Liu for skilled technical assistance with immunohistochemistry.

1. Saltiel, A.R., and Kahn, C.R. 2001. Insulin signaling and the regulation of glucose and lipid metabolism. *Nature*. **414**:799–806.
2. Bell, G.I., and Polonsky, K.S. 2001. Diabetes mellitus and genetically programmed defects in beta-cell function. *Nature*. **414**:788–791.
3. Accili, D. 2001. A kinase in the life of the β cell. *J. Clin. Invest.* **108**:1575–1576. doi:10.1172/JCI200114454.
4. Kulkarni, R.N., et al. 1999. Tissue-specific knock-

out of the insulin receptor in pancreatic β cells creates an insulin secretory defect similar to that in type 2 diabetes. *Cell*. **96**:329–339.

5. Kulkarni, R.N., et al. 2002. Beta-cell-specific deletion of the Igf1 receptor leads to hyperinsulinemia and glucose intolerance but does not alter beta-cell mass. *Nat. Genet.* **31**:111–115.
6. Xuan, S., et al. 2002. Defective insulin secretion in pancreatic β cells lacking type 1 IGF receptor. *J. Clin. Invest.* **110**:1011–1019. doi:10.1172/JCI200215276.
7. Withers, D.J., et al. 1998. Disruption of IRS-2 causes type 2 diabetes in mice. *Nature*. **391**:900–904.
8. Kubota, N., et al. 2000. Disruption of insulin receptor substrate 2 causes type 2 diabetes because of liver insulin resistance and lack of compensatory beta-cell hyperplasia. *Diabetes*. **49**:1880–1889.
9. Kaestner, K.H., Knochel, W., and Martinez, D.E. 2000. Unified nomenclature for the winged helix/forkhead transcription factors. *Genes Dev.* **14**:142–146.
10. Datta, S.R., Brunet, A., and Greenberg, M.E. 1999. Cellular survival: a play in three Akts. *Genes Dev.* **13**:2905–2927.
11. Zhao, H.H., et al. 2001. Forkhead homologue in rhabdomyosarcoma functions as a bifunctional nuclear receptor-interacting protein with both coactivator and corepressor functions. *J. Biol. Chem.* **276**:27907–27912.
12. Nakae, J., et al. 2002. Regulation of insulin action and pancreatic beta-cell function by mutated alleles of the gene encoding forkhead transcription factor *Foxo1*. *Nat. Genet.* **32**:245–253.
13. Nakae, J., Kitamura, T., Silver, D.L., and Accili, D. 2001. The forkhead transcription factor Foxo1 (Fkhr) confers insulin sensitivity onto glucose-6-phosphatase expression. *J. Clin. Invest.* **108**:1359–1367. doi:10.1172/JCI200112876.
14. Kitamura, T., et al. 2001. Preserved pancreatic beta-cell development and function in mice lacking the insulin receptor-related receptor. *Mol. Cell. Biol.* **21**:5624–5630.
15. Marshak, S., et al. 2000. Functional conservation of regulatory elements in the pdx-1 gene: PDX-1 and hepatocyte nuclear factor 3beta transcription factors mediate beta-cell-specific expression. *Mol. Cell. Biol.* **20**:7583–7590.
16. Schreiber, E., Matthias, P., Muller, M.M., and Schaffner, W. 1989. Rapid detection of octamer binding proteins with 'mini-extracts', prepared from a small number of cells. *Nucleic Acids Res.* **17**:6419.
17. Nakae, J., Park, B.-C., and Accili, D. 1999. Insulin stimulates phosphorylation of the forkhead transcription factor FKHR on serine 253 through a wortmannin-sensitive pathway. *J. Biol. Chem.* **274**:15982–15985.
18. Stoffers, D.A., Heller, R.S., Miller, C.P., and Habener, J.F. 1999. Developmental expression of the homeodomain protein IDX-1 in mice transgenic for an IDX-1 promoter/lacZ transcriptional reporter. *Endocrinology*. **140**:5374–5381.
19. Sun, X.J., et al. 1997. The IRS-2 gene on murine chromosome 8 encodes a unique signaling adapter for insulin and cytokine action. *Mol. Endocrinol.* **11**:251–262.
20. Withers, D.J., et al. 1999. Irs-2 coordinates Igf-1 receptor-mediated beta-cell development and peripheral insulin signaling. *Nat. Genet.* **23**:32–40.

21. Bonner-Weir, S. 2000. Life and death of the pancreatic beta cells. *Trends Endocrinol. Metab.* **11**:375–378.
22. Medema, R.H., Kops, G.J., Bos, J.L., and Burgering, B.M. 2000. AFX-like Forkhead transcription factors mediate cell-cycle regulation by Ras and PKB through p27kip1. *Nature*. **404**:782–787.
23. Brunet, A., et al. 1999. Akt promotes cell survival by phosphorylating and inhibiting a forkhead transcription factor. *Cell*. **96**:857–868.
24. Dijkers, P.F., Medemadagger, R.H., Lammers, J.J., Koenderman, L., and Coffey, P.J. 2000. Expression of the pro-apoptotic Bcl-2 family member Bim is regulated by the forkhead transcription factor FKHR-L1. *Curr. Biol.* **10**:1201–1204.
25. Brissova, M., et al. 2002. Reduction in pancreatic transcription factor PDX-1 impairs glucose-stimulated insulin secretion. *J. Biol. Chem.* **277**:11225–11232.
26. Kim, S.K., et al. 2002. Pbx1 inactivation disrupts pancreas development and in *lplf1*-deficient mice promotes diabetes mellitus. *Nat. Genet.* **30**:430–435.
27. Kushner, J.A., et al. 2002. Pdx1 restores β cell function in *Irs2* knockout mice. *J. Clin. Invest.* **109**:1193–1201. doi:10.1172/JCI200214439.
28. Sharma, S., et al. 1997. Hormonal regulation of an islet-specific enhancer in the pancreatic homeobox gene STF-1. *Mol. Cell. Biol.* **17**:2598–2604.
29. Wu, K.L., et al. 1997. Hepatocyte nuclear factor 3beta is involved in pancreatic beta-cell-specific transcription of the *pdx-1* gene. *Mol. Cell. Biol.* **17**:6002–6013.
30. Lee, C., et al. 2002. Foxa2 controls Pdx1 gene expression in pancreatic beta-cells in vivo. *Diabetes*. **51**:2546–2551.
31. Conlon, J.M., Rouiller, D., Boden, G., and Unger, R.H. 1979. Characterization of immunoreactive components of insulin and somatostatin in canine pancreatic juice. *FEBS Lett.* **105**:23–26.
32. Williams, J.A., and Goldfine, I.D. 1985. The insulin-pancreatic acinar axis. *Diabetes*. **34**:980–986.
33. Pour, P. 1978. Islet cells as a component of pancreatic ductal neoplasms. I. Experimental study: ductular cells, including islet cell precursors, as primary progenitor cells of tumors. *Am. J. Pathol.* **90**:295–316.
34. Bertelli, E., Regoli, M., Orazioli, D., and Bendant, M. 2001. Association between islets of Langerhans and pancreatic ductal system in adult rat. Where endocrine and exocrine meet together? *Diabetologia*. **44**:575–584.
35. Guz, Y., Nasir, I., and Teitelman, G. 2001. Regeneration of pancreatic beta cells from intra-islet precursor cells in an experimental model of diabetes. *Endocrinology*. **142**:4956–4968.
36. Movassat, J., Saulnier, C., and Portha, B. 1997. Insulin administration enhances growth of the beta-cell mass in streptozotocin-treated newborn rats. *Diabetes*. **46**:1445–1452.
37. Bonner-Weir, S., et al. 2000. In vitro cultivation of human islets from expanded ductal tissue. *Proc. Natl. Acad. Sci. USA*. **97**:7999–8004.
38. Gu, G., Dubauskaite, J., and Melton, D.A. 2002. Direct evidence for the pancreatic lineage: NGN3+ cells are islet progenitors and are distinct from duct progenitors. *Development*. **129**:2447–2457.